Supporting Information

Electrocatalytic CO_2 Reduction by $M(bpy\text{-}R)(CO)_4$ (M = Mo, W; R = H, *t*Bu) Complexes. Electrochemical, Spectroscopic, and Computational Studies and Comparison with Group 7 Catalysts.

Melissa L. Clark,[a] Kyle A. Grice, [‡a] Curtis E. Moore, Arnold L. Rheingold and Clifford P. Kubiak*

Department of Chemistry and Biochemistry, University of California
San Diego, 9500 Gilman Drive MC 0358, La Jolla, California 92093, USA.
E-mail: ckubiak@ucsd.edu
Fax: 01 858 534 5383
Tel: 01 858 822 2665

I. Experimental

Materials and Methods

Unless otherwise noted, all transformations and manipulations were performed under an atmosphere of N_2 or Ar using standard Schlenk and glovebox techniques. Acetonitrile, pentane, toluene, and tetrahydrofuran (THF) were dried on a custom solvent purification system and stored over 3Å molecular sieves. Complexes **1**, **2**, and **3** were synthesized according to literature methods and spectroscopic data matched literature values.[1,2] Potassium graphite (KC_8) was synthesized according to literature procedures and stored in the glovebox freezer prior to use.[3] Tetrabutylammonium hexafluorophosphate ($TBAPF_6$) was recrystallized from methanol and dried under vacuum. All other reagents and solvents were purchased from commercial suppliers and used as received. FT-IR data was collected on a Thermo Nicolet 6700. ^1H and ^{13}C NMR spectra were collected on a Varian 400 MHz spectrometer or Bruker Avance III 300 MHz spectrometer equipped with a broad band probe. NMR data was referenced against residual solvent peaks and reported downfield of tetramethylsilane (δ = 0 ppm). Elemental analyses were performed by Midwest Microlab, LLC in Indianapolis, IN.

Synthesis of W(4,4'-di-*tert*-butyl-2,2'-bipyridine)(CO)$_4$ (4)

A stirring 15 mL toluene solution of 4,4'-di-*tert*-butyl-2,2'-bipyridine (352 mg, 1.31 mmol) and $W(CO)_6$ (404 mg, 1.15 mmol) was refluxed for 17 h. The solution was filtered through a plug of basic alumina, which was rinsed 3 times with 30 mL dichloromethane. The combined solvent was removed under vacuum and the solid was collected on a filter and rinsed 3 times with 20 mL of pentane to yield a dark red solid (488 mg, 75.3% yield). ^1H NMR (400 MHz, $CDCl_3$): δ = 1.44 (s, 18H), 7.37 (dd, J = 2.2 Hz, J = 5.9 Hz, 2H), 8.07 (br d, J = 1.1 Hz, 2H), 9.09 (d, J = 5.9 Hz, 2H).^1H NMR (400 MHz, THF-d_8): δ = 1.45 (s, 18H), 7.58 (dd, J = 2.0 Hz, J = 6.0 Hz, 2H), 8.40 (br d, J = 2.2 Hz, 2H), 9.10 (d, J = 5.9 Hz, 2H).$^{13}C\{^1H\}$ NMR (100.6 MHz, $CDCl_3$): 30.52, 35.56, 119.09, 123.44, 152.68, 155.84, 162.05, 201.53, 215.85.$^{13}C\{^1H\}$ NMR (100.6 MHz, THF-d_8): 30.25, 36.01, 120.54, 124.22, 153.14, 156.72, 162.93, 202.39, 215.40.Anal Calc. for $C_{22}H_{24}WN_2O_4$: C, 46.81; H, 4.29; H, 4.97. Found: C, 46.78; H, 4.44; N, 4.81.

Synthesis of [W(2,2'-bipyridine)(CO)$_4$][K(18-crown-6)] (5)

Similar to the analogous reductions of Re(bpy-*t*Bu)(CO)$_3$Cl in THF,[4] 20 mL of 3 mM **2** and 18-crown-6 (1.1 equiv) in THF was cooled to –35 ºC. KC_8 (1.1 equiv) was then added to the solution and shaken, in which the solution turned from red to dark orange. The solution was allowed to warm to room temperature (~30 minutes) upon which it was filtered to afford a dark orange solution of the anion. The solvent was removed under reduced pressure, rinsed twice with 1 mL of pentane, then dried under vacuum to yield a black orange solid in 45% yield. X-ray quality crystals were grown from the vapour diffusion of pentane into a portion of a 3 mM THF solution of **5**. IR (THF) ʋ(CO): 1984 cm^{-1}, 1857 cm^{-1}, 1838 cm^{-1}, 1800 cm^{-1}.

Synthesis of [W(4,4'-di-*tert*-butyl-2,2'-bipyridine)(CO)$_3$][K(18-crown-6)]$_2$ (6)

Complex **6** was synthesized and characterized in a similar fashion to **5**, using a 3 mM of **4** in THF, 2.2 equivalents 18-crown-6 (for X-ray and FTIR) and 2.2 equivalents of KC_8 to yield a dark purple solution of **6**. Upon drying a black purple solid was obtained with a yield of 73%. ^1H NMR (300 MHz, THF-d_8): δ = 1.12 (s, 18H), 4.80 (d, J = 6.0 Hz, 2H), 6.60 (d, 2H), 8.47 (d, J = 6.0 Hz, 2H). IR (THF) ʋ(CO): 1837 cm^{-1}, 1713 cm^{-1}.

Synthesis of [W(4,4'-di-*tert*-butyl-2,2'-bipyridine)(CO)$_3$][K(18-crown-6)]

The di-tert-butyl monoanion was synthesized and characterized in a similar fashion to **5**, using 10 mL of 2 mM **4** in THF, 1.1 equivalents 18-crown-6 and 1.1 equivalents of KC_8 to yield a dark orange solution. The black orange solid was collected with a yield of 43%. IR (THF) ʋ(CO): 1982 cm$^{–1}$, 1854 cm$^{–1}$, 1835 cm$^{–1}$, and 1798 cm$^{–1}$.

Synthesis of [W(2,2'-bipyridine)(CO)$_3$][K(18-crown-6)]$_2$

The tungsten bipyridine dianion was synthesized and characterized in a similar fashion to **5**, using a 2 mM of **2** in THF, 2.5 equivalents 18-crown-6 and 2.2 equivalents of KC_8 to yield a dark purple solution. The black purple solid was collected with a yield of 55%. ^1H NMR (300 MHz, THF-d_8): δ = 4.69 (br, 2H), 5.46 (br, 2H), 6.67 (br, 2H), 8.44 (br, 2H). IR (THF) ʋ(CO): 1840 cm^{-1} and 1711 cm^{-1}.

Electrochemistry

Electrochemical experiments were performed with a BAS CV-50W or BAS Epsilon potentiostat using a single-compartment cell. A 1 mm diameter glassy carbon electrode, Pt wire counter electrode, and Ag/AgCl reference electrode (separated from the solution by a vycor tip) were used for all experiments. Cyclic voltammograms were performed at room temperature under N_2 or CO_2 in an acetonitrile solution of 0.1 M $TBAPF_6$ as the electrolyte, which was purged with N_2 or CO_2 before each experiment. The scan rate for cyclic voltammetry was 100 mV·s^{-1} unless otherwise noted. Decamethylferrocene (Fc*) was used as the internal reference, which was then used to reference to SCE.

Bulk Electrolysis

Bulk electrolysis experiments were performed using a BAS Epsilon potentiostat connected to a 60 mL single-compartment cell designed on our laboratory. A 1 mm glassy carbon working electrode, Pt wire counter electrode surrounded by a glass rod (open at the end), and a Ag/AgCl reference electrode protected by a vycor tip was used in the setup. The bulk reductions were performed on a 30 mL scale with a catalyst concentration (4) of 1 mM and 0.1 M $TBAPF_6$. The solution before each experiment was purged with either dry N_2 or CO_2 gas. Gas analyses were performed on a Hewlett-Packard 7890A Series gas chromatograph with two molsieve columns (30 m × 0.53 mm ID × 25 μm film). The injected 1 mL sample of the cell's head was split between the two columns which differed by their carrier gas (N_2 and He) and allowed for quantification of both CO and H_2 in each run. The volume of CO or H_2 was elucidated from the peak area, correlated by gas chromatography calibration curves.

X-Ray Crystallography

Single crystal X-ray diffraction studies were carried out on a Bruker Kappa APEX-II CCD diffractometer equipped with Mo Kα radiation (λ = 0.71073 Å) or a Bruker Kappa APEX CCD diffractometer equipped with Cu Kα radiation (λ = 1.54184 Å). The crystals were mounted on a Cryoloop with Paratone oil and data were collected under a nitrogen gas stream at 100(2) K using ω and ϕ scans. Data were integrated using the Bruker SAINT software program and scaled using the SADABS software program. Solution by direct methods (SHELXS) produced a complete phasing model consistent with the proposed structure. All non-hydrogen atoms were refined anisotropically by full-matrix least-squares (SHELXL-97).[5] All hydrogen atoms were placed using a riding model. Their positions were constrained relative to their parent atom using the appropriate HFIX command in SHELXL-97. Crystallographic data for complexes **3**, **4**, **5**, and **6** are summarized in Table S3.

Density Functional Theory Calculations

Density functional theory (DFT) calculations were performed with the Amsterdam Density Functional (ADF) program suite,[6, 7] version 2012.01.[8] The triple-ζ Slater-type orbital TZ2P ADF basis set was utilized without frozen cores. Relativistic effects were included through use of the zeroth-order regular approximation (ZORA).[9, 10] The functional used was BP86, and the local density approximation (LDA) of Vosko, Wilk and Nusair[11] (VWN) was coupled with the generalized gradient approximation (GGA) corrections described by Becke[12] and Perdew[13, 14] for electron exchange and correlation. Single point frequency calculations were performed to verify that the calculated geometries were at their minima. Molecular orbitals and final geometries were visualized with the ADF-GUI.

References

1. T. S. A. Hor and S.-M. Chee, *Journal of Organometallic Chemistry*, 1987, **331**, 23-28.
2. T. Daniel, N. Suzuki, K. Tanaka and A. Nakamura, *J. Organomet. Chem.*, 1995, **505**, 109-117.
3. M. A. Schwindt, T. Lejon and L. S. Hegedus, *Organometallics*, 1990, **9**, 2814-2819.
4. J. M. Smieja, E. E. Benson, B. Kumar, K. A. Grice, C. S. Seu, A. J. M. Miller, J. M. Mayer and C. P. Kubiak, *Proc. Natl. Acad. Sci. USA*, 2012, **109**, 15646-15650.
5. G. Sheldrick, *Acta Crystallogr., Sect. A*, 2008, **64**, 112.
6. G. te Velde, F. M. Bickelhaupt, E. J. Baerends, C. Fonseca Guerra, S. J. A. van Gisbergen, J. G. Snijders and T. Ziegler, *J. Comput. Chem.*, 2001, **22**, 931.
7. C. Fonseca Guerra, J. G. Snijders, G. te Velde and E. Baerends, *J. Theor. Chem. Acc.*, 1998, **99**, 391.
8. ADF 2012.01, Theoretical Chemistry, Vrije Universiteit, Amsterdam, The Netherlands.
9. E. van Lenthe, E. J. Baerends and J. G. Snijders, *J. Chem. Phys.*, 1993, **99**, 4597.
10. E. van Lenthe, J. G. Snijders and E. J. Baerends, *J. Chem. Phys.*, 1996, **105**, 1200.
11. S. H. Vosko, L. Wilk and M. Nusair, *Can. J. Phys.*, 1980, **58**, 1200.
12. A. D. Becke, *Phys. Rev. A*, 1988, **38**, 3098.
13. J. P. Perdew, *Phys. Rev. B*, 1986, **33**, 8822.
14. J. P. Perdew, *Phys. Rev. B*, 1986, **34**, 7406.
15. S. S. Braga, A. C. Coelho, I. S. Goncalves and F. A. Almeida Paz, *Acta Crystallographica Section E*, 2007, **63**, m780-m782.
16. Q. Ye, Q. Wu, H. Zhao, Y.-M. Song, X. Xue, R.-G. Xiong, S.-M. Pang and G.-H. Lee, *Journal of Organometallic Chemistry*, 2005, **690**, 286-290.
17. J. Chapman, G. Kolawole, N. Long, A. J. P. White, D. J. Williams and P. O'Brien, *S. Afr. J. Sci.*, 2005, **101**, 454-456.

II. Figures and Tables

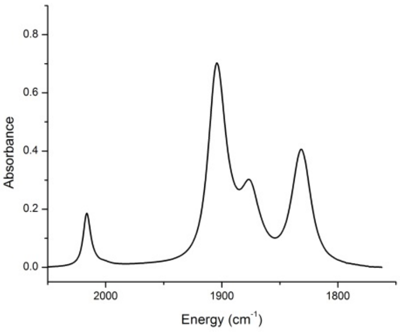

Figure S1. Carbonyl stretching region of the FT-IR spectrum of complex **1** in acetonitrile solution. Complexes **2**–**4** display similar patterns in this region (see Table S1). Complex **1** has υ(CO) stretches at 2016 cm^{-1}, 1904 cm^{-1}, 1877 cm^{-1}, and 1832 cm^{-1}.

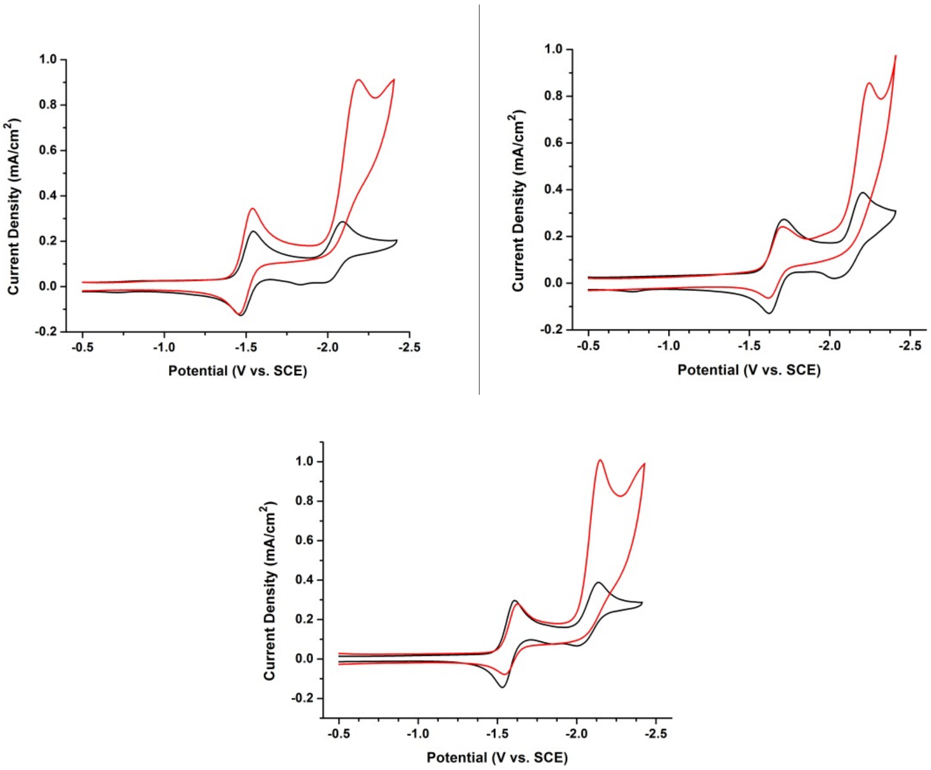

Figure S2.Cyclic voltammograms of complexes **2** (left), **3** (right), and **4** (bottom).

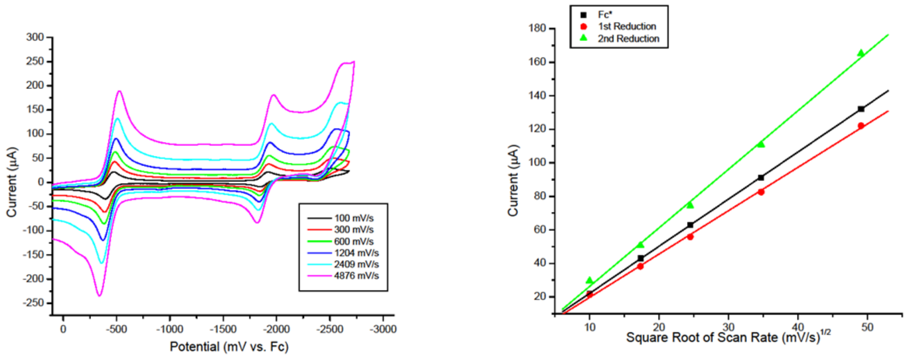

Figure S3. Left: Scan-rate dependence of complex **4** showing $FeCp_2$* along with the first and second reductions at various scan rates. Right: Plot of peak current versus square root of scan rate from scan-rate dependence studies of complex **4**.

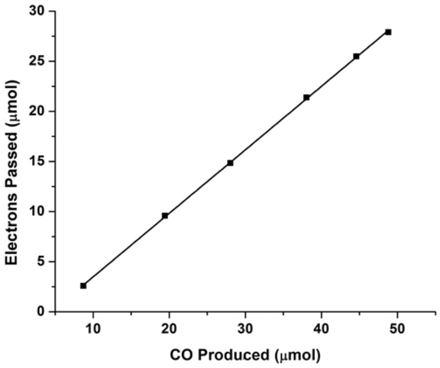

Figure S4. Faradaic efficiency study of W(bpy-*t*Bu)$(CO)_4$ (**4**) in dry acetonitrile with carbon dioxide at -2.3 V. Slope corresponds to 109 ± 7% Faradaic efficiency for the conversion of CO_2 to N_2. This is uncorrected for the amount of CO produced for the loss of a carbonyl ligand upon the second reduction.

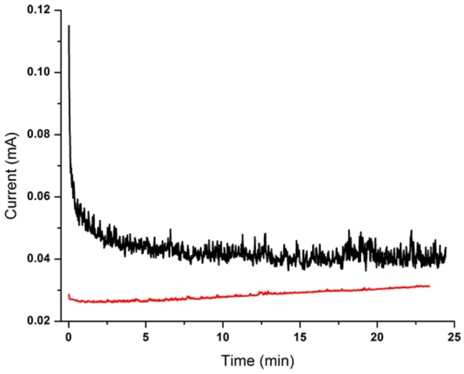

Figure S5. Comparison of current versus time graphs from bulk electrolyses of **4** under N_2 (red) and CO_2 (black) over 24 minutes.

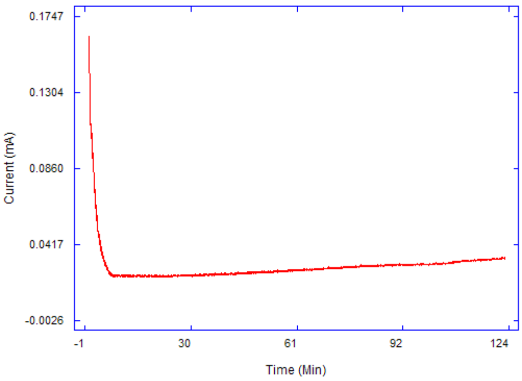

Figure S6. Current versus time graph for the bulk electrolysis of complex **4** under CO_2. The total charge passed was 0.2128 C and the lowest current passed was 0.023 mA at ca. 7 min into the two hour experiment. Experiments of up to 12 hours have been performed and show similar behaviour.

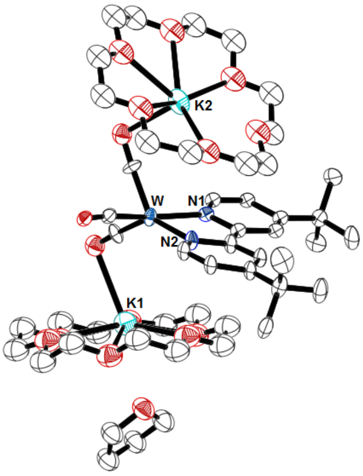

Figure S7. Molecular structure of $[W(bpy\text{-}t\text{Bu})(CO)_3][K(18\text{-crown-}6)]_2\bullet THF$ (**6**) with hydrogen atoms and disorder omitted for clarity. Ellipsoids are shown at 50% probability. The crystal exhibits two-positional disorder across a mirror plane.

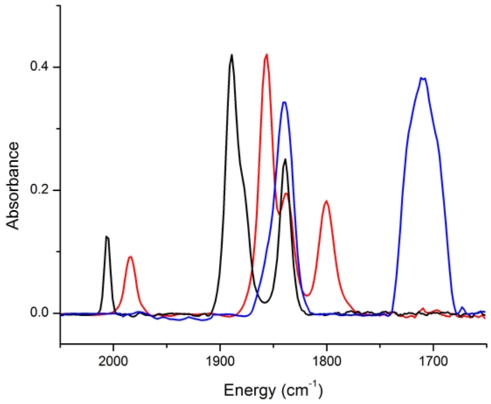

Figure S8. The υ(CO) stretches in the infrared spectra of $W(bpy)(CO)_4$ (**2**) (black), chemically reduced anionic $[W(bpy)(CO)_4][K(18\text{-crown-}6)]$ (**5**) (red), and chemically reduced dianionic $[W(bpy)(CO)_3][K(18\text{-crown-}6)]_2$ (blue). Spectra taken in THF under N_2**.** Neutral species 2 has υ(CO) stretches at 2005 cm^{-1}, 1889 cm^{-1}, and 1839 cm^{-1}. Complex 5 has υ(CO) stretches at 1984 cm^{-1}, 1857 cm^{-1}, 1838 cm^{-1}, and 1800 cm^{-1}. The dianion has stretching frequencies at 1840 cm^{-1} and 1711 cm^{-1}.

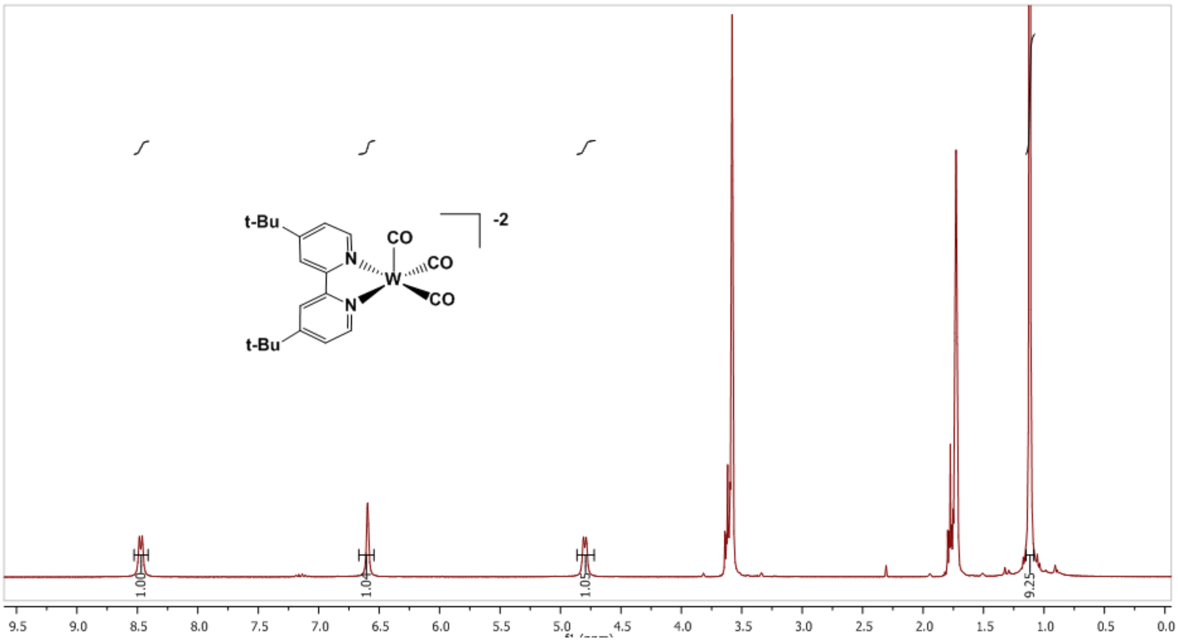

Figure S9. ^{1}H NMR spectrum of [W(4,4'-di-tert-butyl-2,2'-bipyridine)$(CO)_3$][K(18-crown-6)]$_2$ (**6**) in THF-d_8. Solvent residual signals at 1.72 and 3.58 ppm.

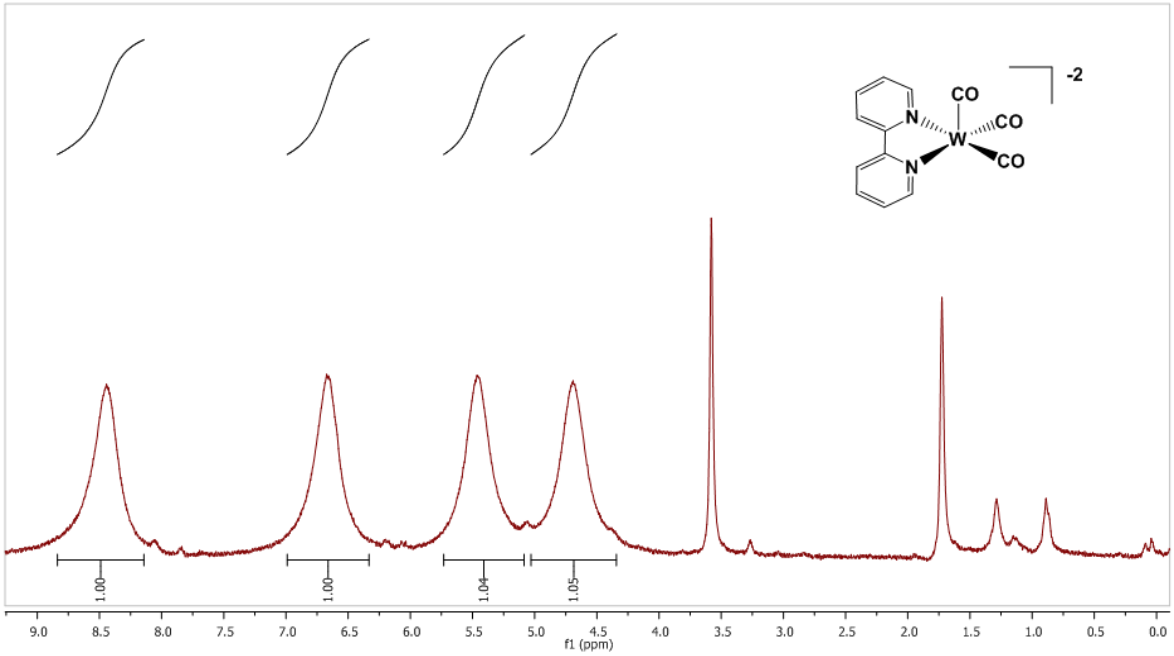

Figure S10. ^{1}H NMR spectrum of [W(2,2'-bipyridine)$(CO)_3$][K(18-crown-6)]$_2$ in THF-d_8. Solvent residual signals at 1.72 ppm and 3.58 ppm for THF- d_8 and peaks at 0.89 ppm and 1.29 ppm are from residual pentane. Peak broadening is likely due to decomposition of the sample (observed by a color change of the solution from dark purple to orange as the signals disappeared).

Table S1. Carbonyl ligand stretching frequencies (cm^{-1}) of $M(L)(CO)_4$ complexes **1–4** in acetonitrile solution.

1	**2**	**3**	**4**
2016	2009	2015	2007
1904	1892	1901	1888
1877	1873[a]	1875	1870[a]
1832	1828	1830	1826

[a] This signal overlaps with the larger signal at higher wavenumbers

Table S2. Selected bond lengths (Å) and angles (deg) for complexes **1-6.**

Bond/Angle	**3**	**1**[15]	**4**	**2**[16, 17]	**5**	**6**
M–N1	2.232(2)	2.249(3)	2.2208(19)	2.272(8)	2.215(3)	2.154(9)
M–N2	2.242(2)	2.241(2)	2.230(2)	2.261(8)	2.212(3)	2.133(9)
M–C1	2.041(3)	2.022(4)	2.041(3)	2.032(11)	2.025(4)	1.892(2)
M–C2	1.964(3)	1.952(4)	1.969(2)	1.938(10)	1.975(4)	1.947(13)
M–C3	1.953(3)	1.962(3)	1.955(3)	1.933(11)	1.961(4)	1.892(7)
M–C4	2.052(3)	2.056(4)	2.037(3)	2.000(11)	2.023(4)	-
C9–C10	1.483(4)	1.483(5)	1.481(3)	1.48(1)	1.396(6)	1.369(14)
N1–M–N2	71.99(8)	72.34(9)	72.12(7)	71.4(3)	73.3(1)	73.1(3)
N1–M–C3	99.93(9)	98.4(1)	99.28(4)	97.1(4)	99.1(1)	98.1(7)
C3–M–C2	89.1(1)	90.1(1)	90.18(10)	93.3(5)	84.6(2)	84.6(6)
C2–M–N2	99.02(9)	99.1(1)	98.46(9)	98.2(4)	103.0(1)	93.6(5)
C1–M–C4	168.3(1)	167.8(1)	168.28(9)	171.5(4)	172.3(2)	-
M–C1–O1	171.8(2)	170.7(3)	171.6(2)	171(1)	173.5(4)	177.0(7)
M–C2–O2	178.7(2)	178.5(3)	178.0(2)	176(1)	176.5(3)	174.0(14)
M–C3–O3	178.9(2)	178.4(3)	178.6(2)	179(1)	176.8(3)	152(3)
M–C4–O4	170.9(2)	171.9(3)	172.2(2)	171(1)	174.2(3)	-

Table S3. Crystallographic data and refinement information**.**

Compound	**Mo(bpy-*t*Bu)(CO)$_4$**	**W(bpy-*t*Bu)(CO)$_4$**
Empirical Formula	$C_{22}H_{24}MoN_2O_4$	$C_{22}H_{24}N_2O_4W$
Formula Weight	476.37	564.28
Temperature (K)	100(2)	100(2)
Crystal System	orthorhombic	orthorhombic
Space Group	Pbca	Pbca
a (Å)	17.9132(6)	17.8251(9)
b (Å)	11.6738(4)	11.6986(6)
c (Å)	21.3034(8)	21.3193(11)
α (deg)	90	90
β (deg)	90	90
γ (deg)	90	90
V (Å^3)	4454.9(3)	4445.7(4)
Z Value	8	8
ρ *calc* (g/cm^3)	1.421	1.686
m (mm^{-1})	0.617	5.225
Theta range for Data Collection (deg)	5.654 to 50.804	3.82 to 50.76
Independent Reflections	4,099 [R(int) = 0.0386]	4,091 [R(int) = 0.0374]
Data/restraints/parameters	4099/0/268	4091/0/268
Goodness of Fit on F^2	1.060	1.071
R indices (all data) R1, wR2	0.0315, 0.0647	0.0198, 0.0408
Largest diff. peak and hole	0.66 to -0.51	0.76 to -0.46

Compound	**[W(bpy)(CO)$_4$][K(18-crown-6)]**	**[W(bpy-*t*Bu)(CO)$_3$][K(18-crown-6)]$_2$**
Empirical Formula	$C_{30}H_{40}KN_2O_{11}W$	$C_{49}H_{80}K_2N_2O_{16}W$
Formula Weight	827.60	1213.01
Temperature (K)	100(2)	100(2)
Crystal System	monoclinic	orthorhombic
Space Group	P2$_1$/c	Pnma
a (Å)	12.2130(3)	29.9821(16)
b (Å)	18.7469(5)	15.8708(9)
c (Å)	15.4880(4)	11.8370(6)
α (deg)	90	90
β (deg)	107.674(1)	90
γ (deg)	90	90
V (Å^3)	3378.69(15)	5632.5(5)
Z Value	4	4
ρ *calc* (g/cm^3)	1.6269	1.430
m (mm^{-1})	3.601	5.622
Theta range for Data Collection (deg)	3.5 to 50.82	5.896 to 138.088
Independent Reflections	6,209 [R(int) = 0.0336]	5,372 [R(int) = 0.1648]
Data/restraints/parameters	6209/0/405	5372/75/311
Goodness of Fit on F^2	0.731	1.061
R indices (all data) R1, wR2	0.0317; 0.0898	0.0968; 0.1980
Largest diff. peak and hole	1.08 and -0.59	2.145 and -1.172

III. DFT Computations

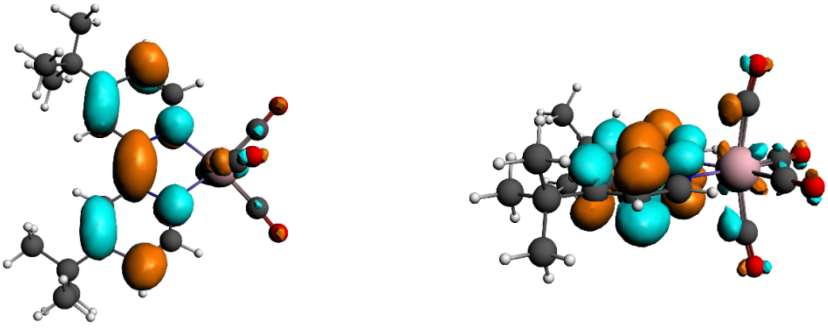

Figure S11. Top and side view of DFT-calculated Lowest Unoccupied Molecular Orbital (LUMO) of W(bpy-*t*Bu)(CO)$_4$ (**A**)

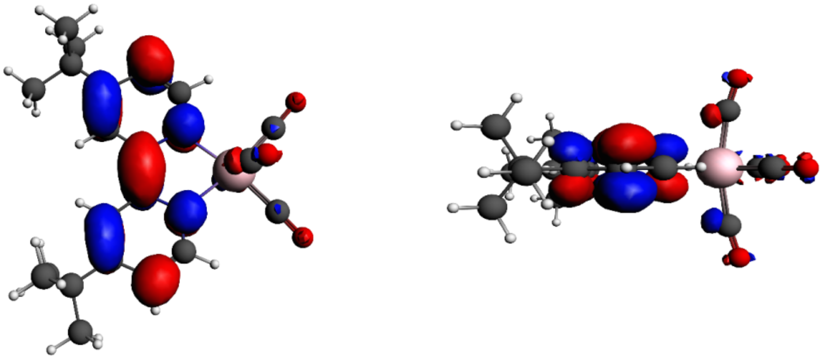

Figure S12. Top and side view of DFT-calculated Singly Occupied Molecular Orbital (SOMO) of [W(bpy-*t*Bu)(CO)$_4$]$^{-1}$ (**B**)

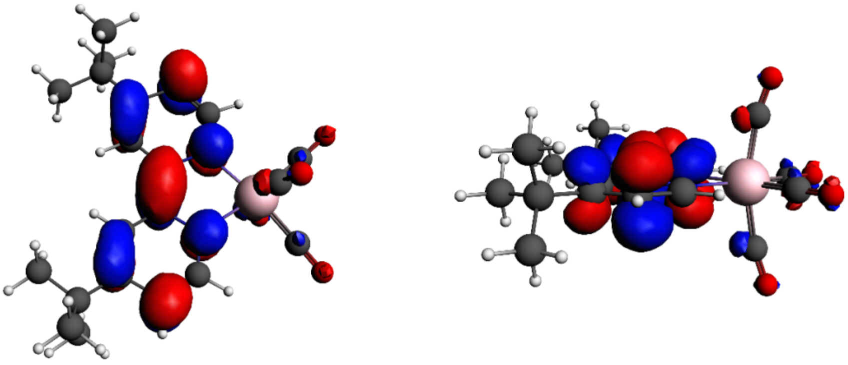

Figure S13. Top and side view of DFT-calculated Highest Occupied Molecular Orbital (HOMO) of [W(bpy-*t*Bu)(CO)$_4$]$^{-2}$ (**C**)

Table S4. Pertinent bond lengths (Å) in the DFT-optimized structures of **A–D.**

Bond	**A**	**B**	**C**	**D**
M–N	2.223	2.234	2.220	2.195
M–N	2.222	2.234	2.220	2.165
M–C$_{ax}$	2.041	2.037	2.037	1.936
M–C$_{ax}$	2.041	2.036	2.037	1.930
M–C$_{eq}$	1.978	1.971	1.972	1.954
M–C$_{eq}$	1.974	1.971	1.971	–
C–O$_{ax}$	1.163	1.170	1.177	1.200
C–O$_{ax}$	1.163	1.170	1.177	1.200
C–O$_{eq}$	1.172	1.181	1.190	1.200
C–O$_{eq}$	1.172	1.181	1.190	–
C$_{py}$–C$_{py}$	1.463	1.423	1.390	1.398
C–N	1.368	1.396	1.432	1.434
C–N	1.364	1.395	1.432	1.422

Table S5. Comparison of the experimental and computational υ(CO) stretching frequencies (in cm^{-1}).

Complex	**Experimental (THF)**	**DFT (gas phase)**
W(bpy-*t*Bu)(CO)$_4$	2004, 1886, 1837	1995, 1912, 1903, 1878
[W(bpy-*t*Bu)(CO)$_4$]$^{-}$	1982, 1854, 1835, 1798	1962, 1864, 1852, 1827
[W(bpy-*t*Bu)(CO)$_4$]$^{2-}$	Not observed	1925, 1814, 1798, 1775
[W(bpy-*t*Bu)(CO)$_3$]$^{2-}$	1837, 1713	1822, 1734, 1724

Table S6. Geometry optimized xyz coordinates for W(bpy-tBu)(CO)$_4$ (**A**) from DFT Calculations

Atom	**X**	**Y**	**Z**
1.W	0.790379	11.179751	7.741391
2.O	-0.704886	8.861315	9.356582
3.O	1.948957	11.855555	10.590981
4.O	2.908110	8.931325	7.126820
5.O	3.111638	13.150460	6.766189
6.N	-0.311931	11.010845	5.819370
7.N	-0.858977	12.669510	7.772876
8.C	-0.245550	9.719468	8.720640
9.C	1.543084	11.581177	9.526710
10.C	2.135586	9.772762	7.387842
11.C	2.208586	12.478475	7.056967
12.C	0.004079	10.130028	4.838517
13.H	0.853193	9.484839	5.045238
14.C	-0.689760	10.035306	3.646784
15.H	-0.362247	9.294848	2.919040
16.C	-1.789027	10.879673	3.388372
17.C	-2.106679	11.783206	4.400230
18.H	-2.940952	12.465143	4.271183
19.C	-1.373310	11.837454	5.593885
20.C	-1.681173	12.763776	6.683851
21.C	-2.732946	13.683558	6.641840
22.H	-3.358290	13.722141	5.753248
23.C	-2.997274	14.547712	7.707981
24.C	-2.141065	14.427881	8.815761
25.H	-2.262795	15.051899	9.697472
26.C	-1.109719	13.501381	8.808416
27.H	-0.441965	13.403715	9.659949
28.C	-2.570847	10.783159	2.073427
29.C	-3.711261	11.813125	2.002194
30.H	-4.447936	11.663227	2.803827
31.H	-4.240715	11.708400	1.045538
32.H	-3.335598	12.844351	2.060692
33.C	-3.179637	9.367424	1.948915
34.H	-2.403738	8.590676	1.957210
35.H	-3.732887	9.281113	1.002330
36.H	-3.875309	9.161088	2.774127
37.C	-1.610955	11.029161	0.886535
38.H	-1.164085	12.031644	0.939373
39.H	-2.161298	10.947634	-0.062138
40.H	-0.795390	10.294622	0.864655
41.C	-4.153811	15.553309	7.634532
42.C	-5.483382	14.795505	7.412816
43.H	-5.472062	14.217892	6.478836
44.H	-6.316102	15.511370	7.352673
45.H	-5.686777	14.100576	8.238962
46.C	-3.918708	16.516408	6.447976
47.H	-2.982347	17.077735	6.571374
48.H	-4.746572	17.237630	6.382490
49.H	-3.867206	15.977900	5.492048
50.C	-4.271110	16.383639	8.923697
51.H	-4.465418	15.750485	9.800227
52.H	-5.108269	17.088811	8.831086
53.H	-3.362690	16.971200	9.114411

Table S7. Geometry optimized *xyz* coordinates for [W(bpy-*t*Bu)(CO)$_4$]$^-$ (**B**) from DFT Calculations

Atom	X	Y	Z
1.W	0.798782	11.179772	7.746514
2.O	-0.713630	8.852339	9.333812
3.O	1.974205	11.806692	10.603045
4.O	2.927328	8.923412	7.190520
5.O	3.147095	13.122251	6.780394
6.N	-0.291653	11.002230	5.805580
7.N	-0.848285	12.688002	7.784914
8.C	-0.262054	9.725672	8.699747
9.C	1.550182	11.557857	9.529513
10.C	2.139832	9.772446	7.420614
11.C	2.218484	12.468471	7.061513
12.C	0.021034	10.149144	4.810810
13.H	0.885751	9.516255	5.000758
14.C	-0.674105	10.043444	3.617111
15.H	-0.335741	9.320274	2.877275
16.C	-1.815937	10.876088	3.395019
17.C	-2.142106	11.754802	4.407532
18.H	-3.000797	12.411477	4.299035
19.C	-1.390072	11.839601	5.613369
20.C	-1.685423	12.746412	6.669269
21.C	-2.752964	13.684338	6.643191
22.H	-3.386675	13.712741	5.758301
23.C	-3.003496	14.552921	7.689831
24.C	-2.129650	14.466273	8.812127
25.H	-2.241725	15.102299	9.685959
26.C	-1.098209	13.536957	8.796870
27.H	-0.421897	13.456266	9.645839
28.C	-2.604534	10.777268	2.082938
29.C	-3.822646	11.716776	2.058918
30.H	-4.527165	11.482324	2.869290
31.H	-4.357786	11.608736	1.103755
32.H	-3.523702	12.769530	2.158179
33.C	-3.109885	9.329564	1.883540
34.H	-2.277865	8.613422	1.864944
35.H	-3.657451	9.242182	0.931250
36.H	-3.785225	9.036708	2.700007
37.C	-1.681341	11.152040	0.900391
38.H	-1.323355	12.186667	0.999822
39.H	-2.222684	11.060845	-0.055279
40.H	-0.801287	10.496333	0.859570
41.C	-4.160228	15.565309	7.608053
42.C	-5.491242	14.831483	7.326721
43.H	-5.451970	14.275355	6.381038
44.H	-6.321371	15.553645	7.261150
45.H	-5.718928	14.113077	8.126533
46.C	-3.891451	16.567639	6.461446
47.H	-2.953101	17.113603	6.632685
48.H	-4.712145	17.300296	6.387517
49.H	-3.805337	16.051055	5.496169
50.C	-4.318613	16.361342	8.916103
51.H	-4.515740	15.697708	9.769196
52.H	-5.163434	17.060863	8.827345
53.H	-3.418311	16.948981	9.141948

Table S8. Geometry optimized *xyz* coordinates for $[\mathrm{W(bpy\text{-}}t\mathrm{Bu)(CO)_4}]^{2-}$ (**C**) from DFT Calculations

Atom	X	Y	Z
1.W	0.794239	11.204635	7.728628
2.O	-0.579831	8.880287	9.447818
3.O	2.055196	11.908638	10.541024
4.O	2.927102	8.928007	7.221305
5.O	3.206857	13.032674	6.688890
6.N	-0.314469	10.960232	5.821107
7.N	-0.835877	12.712138	7.770736
8.C	-0.205449	9.759726	8.760092
9.C	1.587571	11.637077	9.481234
10.C	2.129827	9.787791	7.422444
11.C	2.234748	12.438224	6.985406
12.C	-0.035954	10.074122	4.850969
13.H	0.821175	9.430595	5.054322
14.C	-0.731892	9.926441	3.659771
15.H	-0.410248	9.168043	2.947097
16.C	-1.863717	10.801653	3.410093
17.C	-2.172068	11.717080	4.385447
18.H	-3.008666	12.399749	4.244645
19.C	-1.429700	11.834392	5.615974
20.C	-1.704683	12.741014	6.632661
21.C	-2.787611	13.692711	6.624412
22.H	-3.447049	13.684961	5.757874
23.C	-3.010166	14.582154	7.645843
24.C	-2.095316	14.535508	8.773201
25.H	-2.187107	15.202453	9.629885
26.C	-1.074782	13.595688	8.753798
27.H	-0.383297	13.538245	9.595499
28.C	-2.644703	10.665469	2.097864
29.C	-3.795807	11.678438	1.978037
30.H	-4.523980	11.550185	2.791659
31.H	-4.323367	11.541448	1.019538
32.H	-3.421827	12.711407	2.020801
33.C	-3.247998	9.242681	1.993458
34.H	-2.463610	8.479381	2.090591
35.H	-3.760723	9.098252	1.024974
36.H	-3.973042	9.075074	2.803454
37.C	-1.691479	10.881204	0.896146
38.H	-1.287923	11.904461	0.907623
39.H	-2.217431	10.719999	-0.062450
40.H	-0.838272	10.191055	0.946206
41.C	-4.154005	15.603263	7.645291
42.C	-5.051867	15.496295	6.401065
43.H	-4.477761	15.672102	5.480110
44.H	-5.859388	16.245555	6.450653
45.H	-5.510426	14.499822	6.326810
46.C	-3.573373	17.038521	7.692429
47.H	-2.909263	17.161474	8.559175
48.H	-4.379735	17.791682	7.758113
49.H	-2.977860	17.238853	6.789594
50.C	-5.044441	15.394732	8.895438
51.H	-5.520203	14.403420	8.864624
52.H	-5.835877	16.164110	8.952443
53.H	-4.444752	15.442777	9.814530

Table S9. Geometry optimized *xyz* coordinates for $[W(bpy\text{-}t\text{Bu})(CO)_3]^{2-}$ (**D**) from DFT Calculations

Atom	X	Y	Z
1.W	25.364167	4.045685	2.713676
2.O	23.329082	1.700844	2.325860
3.C	24.081466	2.621903	2.485752
4.O	24.755090	4.074856	5.807524
5.C	24.957760	4.060553	4.624590
6.N	26.250394	4.102924	0.706320
7.N	27.513368	4.105378	2.971538
8.C	25.547637	4.112090	-0.455152
9.H	24.466312	4.103083	-0.321234
10.C	26.094116	4.128471	-1.720567
11.H	25.425081	4.134082	-2.581812
12.C	27.533443	4.131426	-1.869150
13.C	28.270477	4.130900	-0.705621
14.H	29.358954	4.130606	-0.748830
15.C	27.668072	4.124713	0.591474
16.C	28.353777	4.134139	1.809936
17.C	29.772194	4.177327	1.961988
18.H	30.366864	4.202974	1.048873
19.C	30.396033	4.190865	3.188828
20.C	29.520395	4.156736	4.351368
21.H	29.915142	4.161684	5.368451
22.C	28.161334	4.118670	4.177194
23.H	27.498620	4.093881	5.041467
24.C	28.150311	4.126812	-3.271484
25.C	27.700829	5.387664	-4.050410
26.H	26.604907	5.450176	-4.095504
27.H	28.062732	6.297209	-3.548975
28.H	28.091422	5.375360	-5.084136
29.C	29.688026	4.109075	-3.241747
30.H	30.086152	4.992623	-2.722910
31.H	30.065287	3.215891	-2.723768
32.H	30.087466	4.105042	-4.269241
33.C	27.671421	2.876201	-4.050043
34.H	28.012785	1.959233	-3.547806
35.H	26.574377	2.838660	-4.093270
36.H	28.060880	2.878438	-5.084258
37.C	31.911396	4.234260	3.385894
38.C	32.299869	5.480782	4.221328
39.H	33.385316	5.500208	4.429117
40.H	32.028271	6.401067	3.683749
41.H	31.765024	5.490373	5.180919
42.C	32.380651	2.970873	4.151466
43.H	33.466149	3.008516	4.357028
44.H	31.851046	2.876004	5.109547
45.H	32.164822	2.066086	3.564678
46.C	23.865226	5.235569	2.424033
47.C	32.679574	4.295743	2.055125
48.H	33.765136	4.330383	2.244141
49.H	32.468562	3.414066	1.433270
50.H	32.402610	5.189367	1.477775
51.O	22.974622	6.016971	2.232190